

# Visualizing Brain Synchronization: an explainable representation of phase-amplitude coupling

Andrés Ortiz<sup>1,2</sup>, Nicolás J. Gallego-Molina<sup>1,2</sup>, Diego Castillo-Barnes<sup>1,2</sup>, Ignacio Rodríguez-Rodríguez<sup>1,2</sup>, and Juan M. Górriz<sup>3</sup>

<sup>1</sup> Communications Engineering Department  
University of Málaga. 29004 Málaga, Spain

<sup>2</sup> Andalusian Data Science and Computational Intelligence Institute (DaSCI)

<sup>3</sup> Dept. of Signal Theory, Networking and Communications  
University of Granada, Spain [aortiz@ic.uma.es](mailto:aortiz@ic.uma.es)

**Abstract.** In the realm of neuroscience, brain activity is often characterized by rhythmic oscillations at different frequency bands. These oscillations underlie various cognitive processes and constitutes the basis of communication between populations of neurons. Cross-frequency coupling (CFC) refers to techniques directed to study the interactions between oscillations at different frequencies, providing a more comprehensive view of neural dynamics than traditional measures of connectivity or based on the distribution of the power spectral density. In this paper, we propose a method to explore CFC local patterns in an explainable way, allowing to visualize them over time and to easily identify functional brain areas activated during a task development from the Phase-Amplitude Coupling (PAC) point of view.

**Keywords:** Cross-Frequency-Coupling, Phase-Amplitude Coupling, Brain connectivity, Dyslexia

## 1 Introduction

Cross-frequency coupling (CFC) [6] is a phenomenon observed in the brain where the oscillatory activity of neural signals at different frequency bands becomes coordinated or coupled. This intricate interaction provides valuable insights into the functional connectivity of different brain areas and constitutes a crucial aspect in the understanding of the complex dynamics of brain networks. In the field of neuroscience, the brain's activity is often characterized by rhythmic oscillations at different frequency bands (also called neural oscillations [14, 6, 9, 2], such as delta, theta, alpha, beta, and gamma rhythms. These oscillations are thought to underlie various cognitive processes and are essential for communication between different brain regions. Phase-Amplitude coupling (PAC), which is a specific type of CFC, refers to the phenomenon where the phase or amplitude of the oscillations at one frequency is related to the phase or amplitude of oscillations at another frequency. Typically, PAC refers to the modulation

of the higher bands amplitude (e.g. theta) by the phase of lower bands (e.g. gamma). One of the key advantages of studying brain connectivity by means of PAC coupling lies in its ability to unveil details of communication between neurons. This way, the synchronization of higher frequency oscillations in one area with lower frequency oscillations in another area may indicate effective communication between respective populations of neurons. On the other hand, since local neuronal oscillations at different bands imply the processing of different type of information, the long-range interaction between bands is associated to information integration between populations of neurons. As a consequence, PAC can uncover subtle and complex relationships that might be overlooked when only considering single-frequency or classical power-based analyses [18, 3]. Other CFC measures related to PAC are those directed to measure phase consistency between two bands. This is the case of the Phase Locking Value (PLV) [18, 7, 16], which assesses how the phase of a signal (i.e.: lower frequency) is "locked" to the phase of another signal (i.e.: higher frequency) over time. Indeed, PLV allows studying phase synchronization or phase coherence between different brain regions or neuronal populations. Currently, different methods for acquiring functional information due to brain activity are available, such as Electroencephalography (EEG), magnetoencephalography (MEG), Near Infrared Spectrography (NIRS) and Functional Magnetic Resonance Imaging (fMRI). Among these techniques, EEG and MEG are the used in the study of responses to stimuli that requires temporal or spatial resolution, respectively. Moreover, both techniques can be combined for precise source localization. However, the most popular technique due to its accesibility, low cost and non-invasive character is the Electroencephalography (EEG), that can be used to estimate functional connectivity by means of the frequency content of the signals acquired by each sensor.

In this work, we propose a method to extract to extract and study consistent local CFC patterns over time during the application of a stimulus. At the same time, the developed method provides the visualization of the patterns dealing with the explainability and facilitating the discovering of differential patterns among experimental conditions. Our method has been assessed using EEG data from the LEEDUCA database, consisting in controls and dyslexic children under an experiment of modified Auditory Steady-State Response (ASSR) where white noise has been modulated at different frequencies related to the production period of phonemes, syllables and words in spanish. The experiments carried out demonstrated that the proposed method provides discriminant enough features to differentiate between controls and dyslexics, while showing the most relevant brain regions in which PAC is statistically significant. This, in turn, indicates information processing in these areas while the auditory stimulus is applied. The rest of the paper is organized as follows. Section 2 describes the database used in this work and the methods used to calculate and visualize the CFC patterns. Section 4 shows the results and discussion. Finally, 5 draws the conclusions of this work.

## 2 Materials and Methods

### 2.1 The LEEDUCA dataset

The data used in this work was obtained by the LEEDUCA research group at the University of Málaga (Spain) [15, 1]. The LEEDUCA cohort follows more than 1400 children aged 4 to 8 years, applying cognitive and linguistic tasks directed to assess the reading skills[8]. The study was approved by the Medical Ethical Committee of the University of Málaga (05/02/2020 PND016/2020) and supported by the education office of the Junta de Andalucía (regional government) which granted permission to evaluate students at different public schools. The researchers selected an Electroencephalography (EEG) cohort composed of 48 subjects of age 7, 15 of which had clear reading deficit and 33 with no obvious impairment, after evaluation by expert clinicians. These groups had matching age and school-level socio-economic index (SEI). These students were presented an Auditory Steady-State Response (ASSR) stimulus whose amplitude is modulated at 16 Hz (average intra-syllabic rhythm in spanish) [13]. This stimuli was presented in 5 minute sessions over different trials. EEG signals were acquired using Brainvision actiCHamp Plus (battery powered) with actiCAP electrodes (Brain Products GmbH, Germany) in a 32-channel 10-20 configuration optimized for auditory processing, sampled at 500 Hz.

### 2.2 Data preprocessing

EEG preprocessing consisted in the following stages: 1) High-pass filtering using two-ways FIR filter in order to avoid phase distortion with cut-off frequency of 120 Hz. 2) 50 Hz Notch filter, 3) removal of ocular artifacts using Independent Component Analysis (ICA), 5) removal of other artifacts (manually), 6) channel-wise normalization to zero mean and unit variance and 7) baseline correction. In addition, all channels were referenced to  $Cz$  channel. This way, a filtered, multichannel signal  $x_n(t)$  is composed, where  $t$  is the time sample and  $c$  is the channel for each stimulus. Since each stimulus is applied during 5 minutes,  $x_c(t)$  have a total duration of 300 seconds. Subsequently, the signal  $x_c(t)$  is split into 5 seconds, overlapped Hanning windows. Formally, we can express the windowed signal as

$$x_w(t) = x(t - t_k) \cdot w\left(\frac{t - t_k}{T} \cdot (M - 1)\right), \quad t_k = \frac{k \cdot (1 - R) \cdot T}{K - 1} \quad (1)$$

where  $t_k$  is the starting time of the window, and  $w$  is the Hanning window function, defined as

$$w(n) = 0.5 - 0.5 \cos\left(\frac{2\pi n}{M - 1}\right), \quad n = \{0, 1, 2, \dots, M - 1\} \quad (2)$$

In the case of 5 minutes signal and 10 seconds windows with 0.5 overlapping rate, we have 30 overlapped windows. This window duration ensures the capture of Delta band.

### 2.3 Phase-Amplitude Coupling

As explained in the introduction section, PAC refers to the measure of coupling between lower and higher frequencies of a signal  $x(t)$ . Then, computing PAC requires band-pass filtering of the corresponding bands. This filtering is accomplished by 8-pole, two ways Finite Impulse Response (FIR) filter, since it is crucial to avoid phase distortion. Band-pass signals are then used to compute instantaneous phase  $\phi(t)$  from its analytic version  $z(t)$ , which is obtained from the Hilbert transform as

$$z(t) = x(t) + jH[x(t)] \quad (3)$$

where  $H[x(t)]$  corresponds to the Hilbert transform (HT) of the signal  $x(t)$

$$H[x(t)] = \frac{1}{\pi} \int_{-\infty}^{+\infty} \frac{x(\tau)}{t - \tau} d\tau \quad (4)$$

The analytic signal,  $z(t)$  allows us to estimate the instantaneous, unwrapped phase  $\phi(t)$  as

$$\phi(t) = \angle z(t) = \tan^{-1} \frac{\Im(z(t))}{\Re(z(t))} \quad (5)$$

Please note that we avoided the channel sub-index for the sake of clarity in the previous equations. As explained in the previous section, in this work we used PLV as a measure of neuronal synchronization, which has the advantage of immunity to false PAC estimation due to volume conduction. PLV is defined for each window as

$$\frac{1}{N} \sum_n^M |e^{\phi_1(n) - \phi_2(n)}| \quad (6)$$

where  $\phi(1)$  and  $\phi(2)$  are the phase of low frequency and high frequency signals, respectively.

In order to avoid PLV values obtained by chance, a permutation test is performed [16]. This is addressed by generating *surrogates* of the lower frequency signal by shuffling all samples in the window. Using 200 permutations, we can compute the probability of obtaining higher PLV values (corresponding to higher levels of coupling) with the shuffled versions of the lower frequency signal than with the non-shuffled version. In other words, this allows to compute the p-value as a measure of significance of each PLV value.

### 2.4 Visualization of local PAC patterns

PAC is visualized by using a template composed by projecting the location of the EEG electrodes from a 3-D space onto a 2-D surface. This is addressed by an spherical projection which transform 3-D electrode locations into 2-D projected locations as proposed by [5].

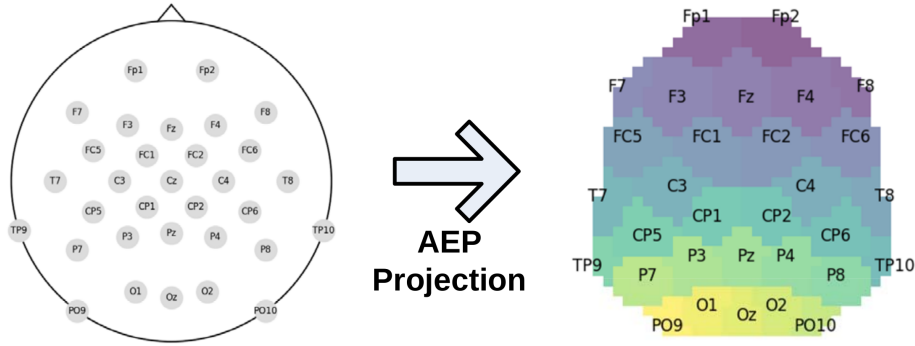


Fig. 1: Azimuthal Equidistant Projection (AEP) from topoplot electrode positions (10-20 international system)

Specifically, we used the Azimuthal Equidistant Projection (AEP) [17] that is widely extended in geographical map projection. This has the property that all points on the map are at proportionally correct distances from the center point (here,  $Cz$ ), and all points on the map are at the correct azimuth (direction) from the center point. Consequently, the projected positions of each electrode are used as centers of a Voronoi tessellation, assigning areas of similar surface to each electrode. Then, PAC values corresponding to each electrode are assigned to the area covered according to the Voronoi set, and subsequently, the image is interpolated to avoid hard transitions between areas. As a result, we obtain the figures in 2

This way, Figure shows the cumulative number of significant PLV values ( $p < 0.05$ ) for each electrode, in order to identify the bands in which the interaction is more statistically significant. As show in this figure, Delta-High Gamma, Theta-High Gamma and Alpha-High Gamma are the pair of bands that can be selected as most relevant.

### 3 Consistency of temporal patterns

As explained before, EEG channel data is split into overlapping windows. In this work, the main aim is to use PAC patterns temporarily consistent, i.e. PAC patterns that remains stable over time, which implies to perform a statistical validation for each signal considering all the time windows. This has been addressed by computing the autocorrelation of the signals for each channel at each time window.

In order to assess the statistical significance of the autocorrelations computed at different windows, we used the (LBQ) test [19], based on the Ljung-Box  $Q$  statistic, defined as:

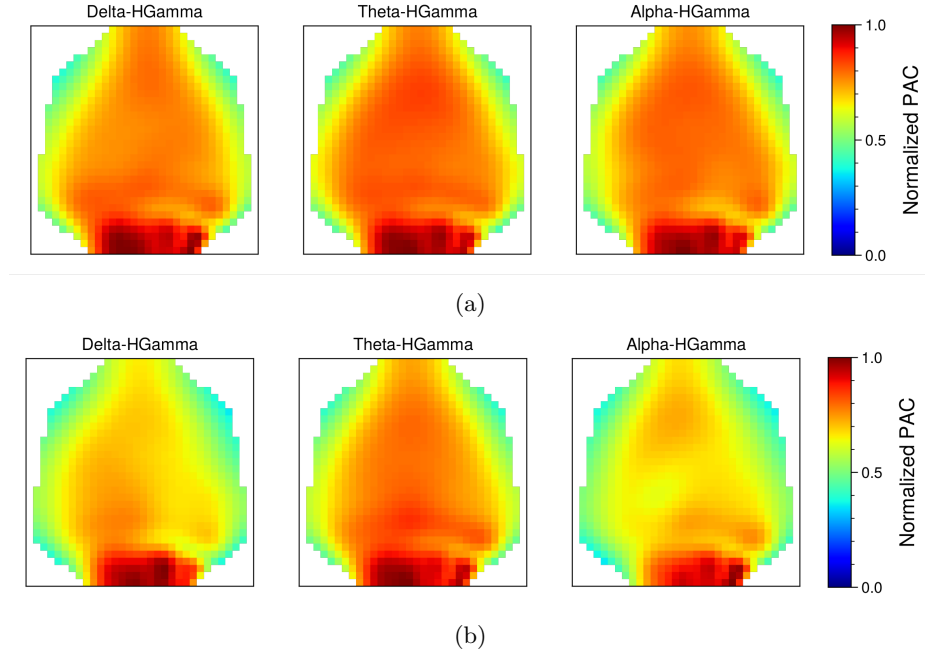


Fig. 2: Visualization of PAC patterns using the proposed method for (a) Controls and (b) Dyslexic subjects

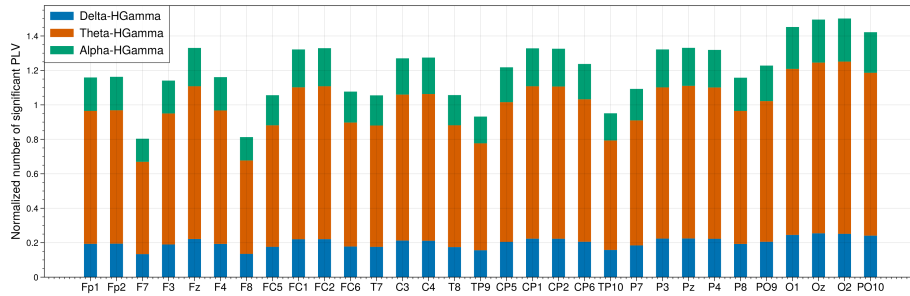


Fig. 3: Number of significant PLV values found at each electrode

$$Q = n(n+2) \sum_{k=1}^h \frac{\hat{r}_k^2}{n-k} \quad (7)$$

where  $n$  is the number of observations in the time series,  $h$  is the number of lags being tested,  $\hat{r}_k$  is the sample autocorrelation at lag  $k$ .

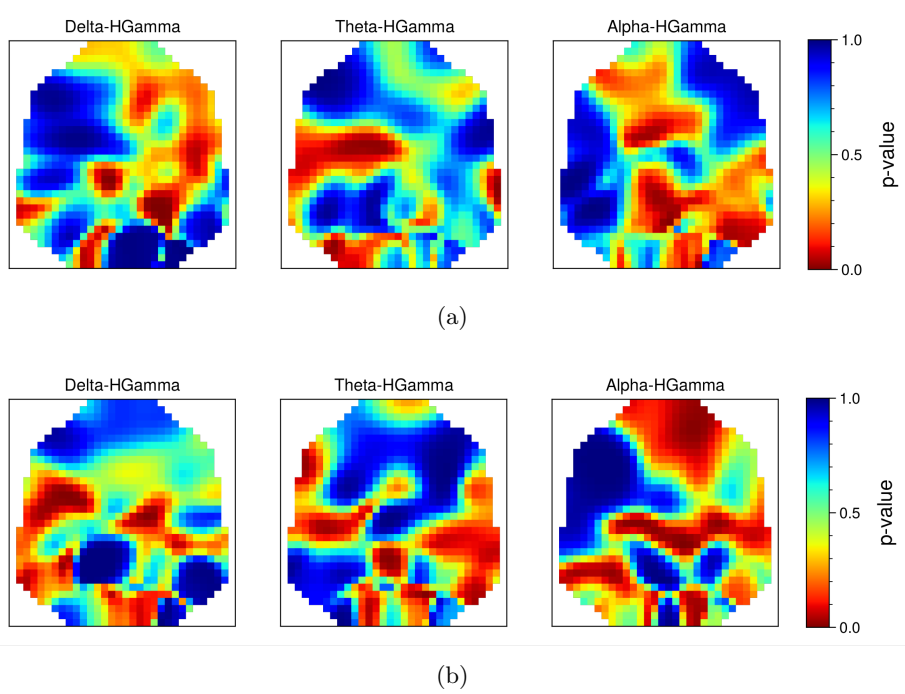


Fig. 4: Temporal significance Map for (a) Controls and (b) Dyslexic subjects

The null hypothesis  $H_0$  for the LBQ test is that the autocorrelations up to lag  $h$  are all equal to zero, i.e.: there is no autocorrelation among time series up to the specified lag order.

Under the null hypothesis, the statistic  $Q$  follows approximately a  $\chi^2$  distribution with degrees of freedom equal to the number of lags  $h$  being tested. The critical values from the chi-squared distribution can be used to determine whether the observed test statistic is statistically significant. The maximum number of lags involves a balance between capturing autocorrelation in the time series and avoiding overfitting, and was chosen as 50% ( $n/2$  samples).

## 4 Results and discussion

In this Section, we show results obtained using a 4.8 Hz ASSR stimulus. Firstly, the number of significant PLV values accounted for each phase-amplitude pair of bands have been accounted at each electrode. This way, Figure 3 depicts the three pair of bands in which a larger number of significant values ( $p < 0.05$ ) have been found. This shows that Theta (phase signal) - High Gamma (amplitude signal) is considerably significant than other bands. Language processing involves the integration of information over different timescales. Indeed, Theta-Gamma coupling may help in binding together relevant information that is distributed across

various neuronal populations and processing stages. The theta phase can act as a temporal reference, enabling the synchronization of gamma oscillations during specific phases to enhance the processing of linguistic information. The presence of discriminant information in this PAC is consistent with the related literature [9, 12], where EEG responses tracked phonetic features of speech provide evidences for impaired low-frequency cortical tracking to phonetic features during natural speech perception. Moreover [4] analyzes neurophysiological signals related to speech processing, focusing on the tracking of amplitude envelope of speech stimuli. According to this, theta-band exhibits greater modulation energy in a lower-frequency band. Additionally, this study also shows that coupling is present in delta and theta bands suggesting its role in the development of speech processing.

Discriminative capabilities of PLV patterns shown in Figure 2 has been evaluated by feeding a gradient boosting classifier [11] in a *Pixels-as-Features* way, but using the temporal significance maps (Figure 4) as a mask. The results obtained are graphically depicted in Figure 5, where Theta-Gamma band exhibits the best area under ROC curve. These results have been assessed using k-fold cross validation scheme (k=5) (error bars in Figure 5 indicates the standard deviation over the k-folds).

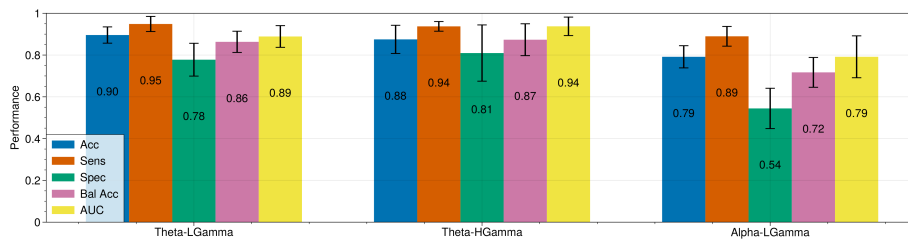


Fig. 5: Classification performance obtained for each PAC band

Since dimensionality of PAC images is considerably larger than the number of available samples [10], an experiment reducing the dimensionality by projecting the images into the 10 first principal components provided by Principal Component Analysis (PCA) has been carried out. These results are also detailed in Table 1.

## 5 Conclusions

In this work, we proposed a method to transform Phase-Amplitude Coupling information from EEG signals into images. This provides an explainable view of the significant cross-frequency couplings found at each electrode, and demonstrates its usefulness when discriminating between controls and dyslexics from local PAC patterns. Indeed, it is possible to visually analyze these patterns,

Pixels-As-Features						
Bands	Acc	Sens 3	Spec	Bal ACC	AUC	
<i>Delta-HGamma</i>	0.84±0.18	0.89±0.11	0.72±0.31	0.80±0.21	0.83±0.20	
<b>Theta-HGamma</b>	0.86±0.11	0.91±0.09	0.73±0.25	0.82±0.16	0.83±0.16	
<i>Alpha-HGamma</i>	0.85±0.05	0.92±0.07	0.73±0.16	0.83±0.07	0.89±0.14	
PCA, 10 components						
Bands	Acc	Sens 3	Spec	Bal ACC	AUC	
<i>Delta-HGamma</i>	0.85±0.08	0.88±0.06	0.77±0.24	0.82±0.14	0.92±0.06	
<b>Theta-HGamma</b>	0.95±0.07	0.97±0.06	0.89±0.14	0.93±0.10	0.93±0.14	
<i>Alpha-HGamma</i>	0.90±0.03	0.91±0.05	0.93±0.13	0.92±0.05	0.91±0.10	

Table 1: Classification results

identifying brain areas of high and low functional activity from the PAC point of view. On the other hand, we use the same idea to analyze the time evolution of PAC patterns in the quest for temporally consistent patterns linked to the processing of the auditory stimulus. The classification results obtained demonstrated that the proposed method is able to capture relevant information from EEG and transforming it into an image, which was the main aim of this work.

## Acknowledgements

This research is part of the PID2022-137461NB-C32, TED2021-132261B-I00, PID2022-137629OA-I00 and PID2022-137451OB-I00 projects, funded by the MCIN/AEI/10.13039/501100011033 and by ESF+ (“NextGenerationEU”/PRTR”) as well as UMA20-FEDERJA-086 (Consejería de Economía y Conocimiento, Junta de Andalucía) and by European Regional Development Funds (ERDF). Work by D.C.B. is supported by the MCIN/AEI/FJC2021-048082-I ‘Juan de la Cierva Formacion’ grant. Work by I.R.-R. is funded by Plan Andaluz de Investigación, Desarrollo e Innovación (PAIDI), Junta de Andalucía.

## References

1. Leeduca project. university of Málaga. [www.leeduca.uma.es](http://www.leeduca.uma.es), accessed: 2024-01-20
2. et al., J.G.: Computational approaches to explainable artificial intelligence: Advances in theory, applications and trends. *Information Fusion* **100**, 101945 (2023). <https://doi.org/https://doi.org/10.1016/j.inffus.2023.101945>, <https://www.sciencedirect.com/science/article/pii/S1566253523002610>
3. et al., J.M.G.: Artificial intelligence within the interplay between natural and artificial computation: Advances in data science, trends and applications. *Neurocomputing* **410**, 237–270 (2020). <https://doi.org/https://doi.org/10.1016/j.neucom.2020.05.078>, <https://www.sciencedirect.com/science/article/pii/S0925231220309292>
4. Attaheri, A., Choidealbha, Á.N., Liberto, G.M.D., Rocha, S., Brusini, P., Mead, N., Olawole-Scott, H., Boutris, P., Gibbon, S., Williams, I., Grey, C., Flanagan, S., Goswami, U.: Delta- and theta-band cortical tracking and phase-amplitude

- coupling to sung speech by infants. *bioRxiv* p. 2020.10.12.329326 (Mar 2021). <https://doi.org/10.1101/2020.10.12.329326>
5. Bashivan, P., Rish, I., Yeasin, M., Codella, N.: Learning Representations from EEG with Deep Recurrent-Convolutional Neural Networks (Feb 2016)
  6. Canolty, R.T., Knight, R.T.: The functional role of cross-frequency coupling. *Trends in cognitive sciences* **14**(11), 506–515 (2010)
  7. Cohen, M.X.: *Analyzing Neural Time Series Data: Theory and Practice* (2014)
  8. De Vos, A., Vanvooren, S., Vanderauwera, J., Ghesquière, P., Wouters, J.: A longitudinal study investigating neural processing of speech envelope modulation rates in children with (a family risk for) dyslexia. *Cortex* **93**, 206–219 (05 2017)
  9. Di Liberto, G.M., Peter, V., Kalashnikova, M., Goswami, U., Burnham, D., Lalor, E.C.: Atypical cortical entrainment to speech in the right hemisphere underpins phonemic deficits in dyslexia. *NeuroImage* **175**, 70–79 (Jul 2018). <https://doi.org/10.1016/j.neuroimage.2018.03.072>
  10. Duin, R.P.: Classifiers in almost empty spaces. In: *Proceedings 15th International Conference on Pattern Recognition. ICPR-2000*. vol. 2, pp. 1–7. IEEE (2000)
  11. Friedman, J.: Greedy function approximation: A gradient boosting machine. *The Annals of Statistics* **29** (11 2000). <https://doi.org/10.1214/aos/1013203451>
  12. Lizarazu, M., Carreiras, M., Molinaro, N.: Theta-gamma phase-amplitude coupling in auditory cortex is modulated by language proficiency. *Human Brain Mapping* **44**(7), 2862–2872 (2023). <https://doi.org/https://doi.org/10.1002/hbm.26250>, <https://onlinelibrary.wiley.com/doi/abs/10.1002/hbm.26250>
  13. Lizarazu, M., Lallier, M., Molinaro, N.: Phaseamplitude coupling between theta and gamma oscillations adapts to speech rate. *Annals of the New York Academy of Sciences* **1453**(1), 140–152 (2019)
  14. Molinaro, N., Lizarazu, M., Lallier, M., Bourguignon, M., Carreiras, M.: Out-of-synchrony speech entrainment in developmental dyslexia. *Human Brain Mapping* **37**, 2767–2783 (08 2016)
  15. Ortiz, A., López, P., Luque, J.L., Martínez-Murcia, F.J., Aquino-Britez, D., Ortega, J.: An anomaly detection approach for dyslexia diagnosis using eeg signals. In: *International Work-Conference on the Interplay Between Natural and Artificial Computation*. pp. 369–378. Springer (2019)
  16. Penny, W., Duzel, E., Miller, K., Ojemann, J.: Testing for nested oscillation. *Journal of Neuroscience Methods* **174**(1), 50–61 (2008). <https://doi.org/https://doi.org/10.1016/j.jneumeth.2008.06.035>, <https://www.sciencedirect.com/science/article/pii/S0165027008003816>
  17. Snyder, J.P.: *Map projections: A working manual*. Tech. Rep. 1395, U.S. Government Printing Office (1987). <https://doi.org/10.3133/pp1395>
  18. Tort, A.B.L., Komorowski, R., Eichenbaum, H., Kopell, N.: Measuring phase-amplitude coupling between neuronal oscillations of different frequencies. *Journal of Neurophysiology* **104**(2), 1195–1210 (2010)
  19. Upton, G., Cook, I.: *A Dictionary of Statistics*. Oxford University Press (2008). <https://doi.org/10.1093/acref/9780199541454.001.0001>, <https://www.oxfordreference.com/view/10.1093/acref/9780199541454.001.0001/acref-9780199541454>